Experimental Thermal and Fluid Science 80 (2017) 376–383

Contents lists available at ScienceDirect

Experimental Thermal and Fluid Science

journal homepage: www.elsevier.com/locate/etfs

A correlation of nanofluid flow boiling heat transfer based on the experimental results of AlN/H_2O and Al_2O_3/H_2O nanofluid

Y. Wang [a], K.H. Deng [b], B. Liu [b], J.M. Wu [b,*], G.H. Su [a]

[a] State Key Laboratory of Multiphase Flow in Power Engineering, School of Nuclear Science and Technology, Xi'an Jiaotong University, Xianning West Road 28#, Xi'an 710049, China
[b] State Key Laboratory for Strength and Vibration of Mechanical Structures, Xi'an Jiaotong University, Xianning West Road 28#, Xi'an 710049, China

ARTICLE INFO

Article history:
Received 27 May 2016
Received in revised form 15 August 2016
Accepted 18 August 2016
Available online 22 August 2016

Keywords:
Nanofluid
Flow boiling
Heat transfer
Correlation

ABSTRACT

Nanofluid flow boiling is becoming a research focus these years, although few correlation of nanofluid flow boiling was proposed in the last researches. In this paper, nanofluid was prepared by adjusting the nanoparticles into the deionized water and dispersing by an ultrasonic oscillation. Nanofluid saturated flow boiling heat transfer in a vertical tube is experimentally investigated in this work. Furthermore, nanoparticle shapes and sizes are scanned by TEM before and after boiling and it has been ensured that the nanoparticles haven't been changed during the experimental process. Several relevant dimensionless parameters for nanofluid saturated flow boiling were proposed to present the influences of heat flux, pressure and thermal properties. Based on the research above, a new correlation for nanofluid saturated flow boiling was presented with 300 experimental points. This correlation apply to both AlN/H_2O nanofluid and Al_2O_3/H_2O nanofluid (0.1–0.5 Vol.%). The pressure range of application for the correlation is 0.2–0.8 MPa, and it is 48–289 kW m^{-2} for heat flux, 350–1100 kg m^{-2} s^{-1} for mass flow rate. The correlation adjust residual sum of squares (A-R^2) is 0.9594. Its mean absolute deviation (MAD) is 4.3% and it predicts 99% of the entire database within ±15% for AlN/H_2O nanofluid and 94.5% of the entire database within ±15% for Al_2O_3/H_2O nanofluid.

1. Introduction

As the requirement of heat transfer capacity for high heat flux system is improved, some new working fluids are proposed like nanofluid [1]. In the first decade after 1995, most researches about nanofluid are its preparation, stability, physical properties and some primary applications [2–7]. Nanofluid convective and pool boiling have been investigated after it was proposed [8–13], however, as flow boiling widely used in the industrial heat transfer system, nanofluid flow boiling heat transfer characteristics were investigated after 2003 [14]. Moreover, nanofluid flow boiling heat transfer enhancement and deterioration are both found in the research under normal pressure. Thereafter, no nanofluid flow boiling research was reported in a few years. In 2009, Peng et al. [15] experimentally investigated nanofluid flow boiling under negative pressure, and it was confirmed that the flow boiling heat transfer capacity of CuO/R113 nanofluid with 0.5 wt% nanoparticles is improved 29.7% compared with base fluid. In the recent years, a growing number of nanofluid flow boiling researches were reported. In 2008, Coursey et al. [16] studied Al_2O_3/ethanol nanofluid flow boiling. It is found that nanoparticle degrades or not has no influence on flow boiling heat transfer.

Kim et al. [17] experimentally studied Al_2O_3/H_2O nanofluid (0.01 Vol.% nanoparticle concentration) flow boiling heat transfer with the consideration of different mass flux and heat flux under atmospheric pressure. It was found that nanofluid flow boiling critical heat flux is enhanced by about 30%. Kim et al. [18] experimentally studied Al_2O_3/H_2O, ZnO/H_2O and diamond/H_2O nanofluid flow boiling heat transfer with 0.001–0.1 Vol.% nanoparticles and 5.53 mm diameter under normal pressure, and it was found that the three kinds of nanofluid flow boiling heat transfer capacity were closed to each other with ±20% deviation in their research. In the same year, Cu/H_2O nanofluid flow boiling was studied by Boudouh et al. [19], and in the tiny channel (diameter of 0.8 mm and length of 160 mm) this kind nanofluid flow boiling heat transfer capacity was enhanced with increasing nanoparticle concentration. In addition, Xu et al. [20] experimentally studied Al_2O_3/H_2O (diameter of 40 nm and concentration of 0.2 wt%) nanofluid flow boiling in a rectangular micro-channel (0.1 mm × 0.25 mm, length of 7.5 mm). It was confirmed that nanofluid flow boiling heat transfer coefficient is much greater than that of pure water. Furthermore, they proposed that the bubble departure size is smaller

* Corresponding author at: School of Aerospace, Xi'an Jiaotong University, Xi'an City 710049, China.
E-mail address: wjmxjtu@mail.xjtu.edu.cn (J.M. Wu).

http://dx.doi.org/10.1016/j.expthermflusci.2016.08.020
0894-1777/

Nomenclature

c_p	specific heat at constant pressure (kJ/kg K)
d	diameter of nanoparticle (m)
D	diameter of test section (m)
F	boiling effect coefficient
G	mass flow rate (kg s^{-1})
h	heat transfer coefficient (W/m K)
h_{fg}	latent heat (J/kg)
J	superficial velocity (m/s)
k	thermal conductivity (W/m k)
l	length of test section
p	pressure (MPa)
N	total data number
Pr	Prandtl number
q	heat flux (W/m^2)
Q	heat (W)
r	radius of test section (m)
R	deviation
Re	Reynolds number
S	boiling inhibition coefficient
x	mass quality
T	temperature (K)

Greek symbols

σ	surface tension (N/m)
ρ	density of nanofluid (kg/m^3)
Φ	heat of unit volume of test section (W/m^3)
μ	dynamic viscosity (kg/m s)
η	thermal efficiency
υ	kinematic viscosity (m^2/s)

Superscripts

c	convection
dau	data acquisition uncertainty
exp	experiment value
g	gas phase
i	thermocouple number
in	inert
j	experimental data number
l	liquid phase
max	maximum value
min	minimum value
muu	measuring unit uncertainty
NB	nuclear boiling
nf	nanofluid
out	outer
p	particle
$pred$	prediction data
s	stainless steel
sat	saturation
w	wall

Abbreviations

CHF	critical heat flux
MAD	mean absolute deviation
RD	relative deviation
SEM	scanning electron microscope
TEM	transmission electron microscope

and the bubble departure frequency is higher in nanofluid. Recently, Rana et al. [21,22] carried out the subcooling flow boiling heat transfer of ZnO/H_2O nanofluid with low nanoparticle concentrations in a horizontal annulus under atmosphere. In their research, the heating surface was observed by scanning election microscope (SEM), and it was found that the heating surface was modified. The heat transfer capacity was increased with increasing the nanoparticle concentration. In 2014, Sun et al. [23] studied the flow boiling heat transfer of four nanofluid (Al/R141b, Cu/R141b, CuO/R141b and Al_2O_3/R141b) in a horizontal tube (inner diameter of 10 mm) under atmosphere, and the heat transfer coefficient nanofluid were increased with increasing mass velocity, mass fraction and quality, moreover, the nanoparticle concentration had the main influence on the nanofluid flow boiling heat transfer. The research on nanofluid flow boiling had mostly been experimentally carried out, numerical studies are rare. Abedini et al. [24] numerically studied the subcooled flow boiling of Al_2O_3/H_2O nanofluid by mixture model. Their results showed that thermal conductivity is the key role for nanofluid heat transfer enhancement. In the other hand, the specific heat and viscosity of nanofluid had no significant influence on nanofluid heat transfer enhancement. Previously, Wang et al. [5] numerically investigated the bubble behavior in nanofluid. It is found that the bubble in nanofluid grows faster and departs from the heating surface earlier, the heat transfer capacity of nanofluid is greater than that of based fluid. It is undeniable that the research of nanofluid on flow boiling heat transfer is inadequate and the experiment data is insufficient for nanofluid application [25]. So far, there is no published research papers on nanofluid flow boiling heat transfer correlation.

In present study, Al_2O_3/H_2O and AlN/H_2O nanofluids flow boiling heat transfer are experimentally investigated in a vertical tube under different pressures. The influence of heat flux and mass flow rate are also under consideration. Moreover, nanoparticle size and shape are observed by transmission electron microscope (TEM) to confirm that nanoparticle have not obviously changed before and after boiling. Relevant dimensionless parameters on nanofluid flow boiling are analyzed and a new correlation for nanofluid flow boiling is proposed.

2. Experiment setup

2.1. Data acquisition and processing

An experimental system was designed and constructed for nanofluid flow boiling heat transfer. The system was constructed of stainless steel, including test section, cooling system and pressure system, as shown in Fig. 1. Moreover, a stainless steel shield pump was used as a power unit, a nanofluid/water tank and an ultrasonic vibration unit to prepare nanofluid and prevent the nanoparticle depositing in the tank.

The test section is a vertical stainless steel tube with 6 mm of inner diameter, 8 mm of outer diameter and 1.1 m of length (as shown in Fig. 2). It is electrically heated by a programmable DC power designed by Ametek-Sorensen. Moreover, the preheating section is also electrically heated by a programmable DC power, and the inlet fluid temperature is controlled by adjusting it. Ten calibrated T-type thermocouple are arranged on the test section outer surface with a 10 mm interval between each other. The inlet and outlet fluid temperatures are measured by two K-type thermocouple, which are installed into the flow.

Thermal insulation materials are surrounded on the test section to minimize the heat loss and the thermal efficiency can reach over

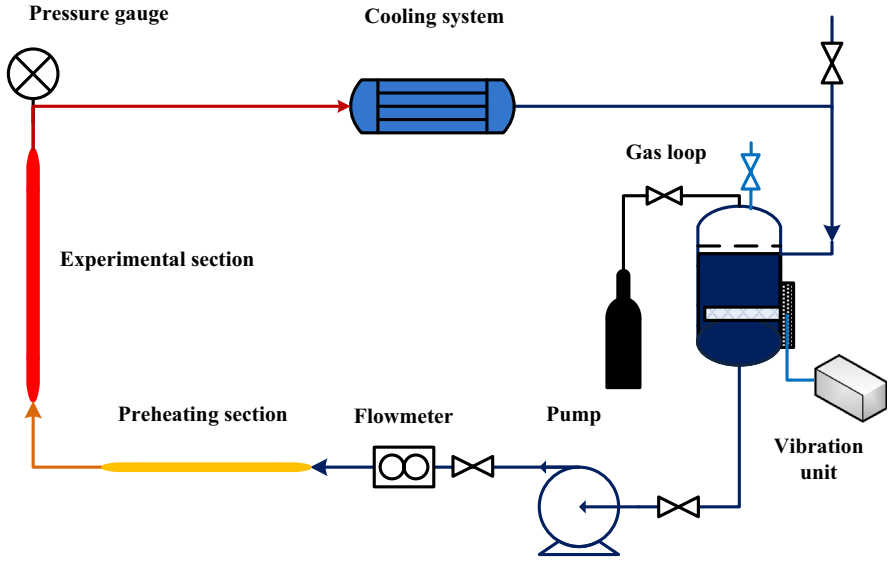

Fig. 1. Nanofluid flow boiling heat transfer experimental system schematic diagram.

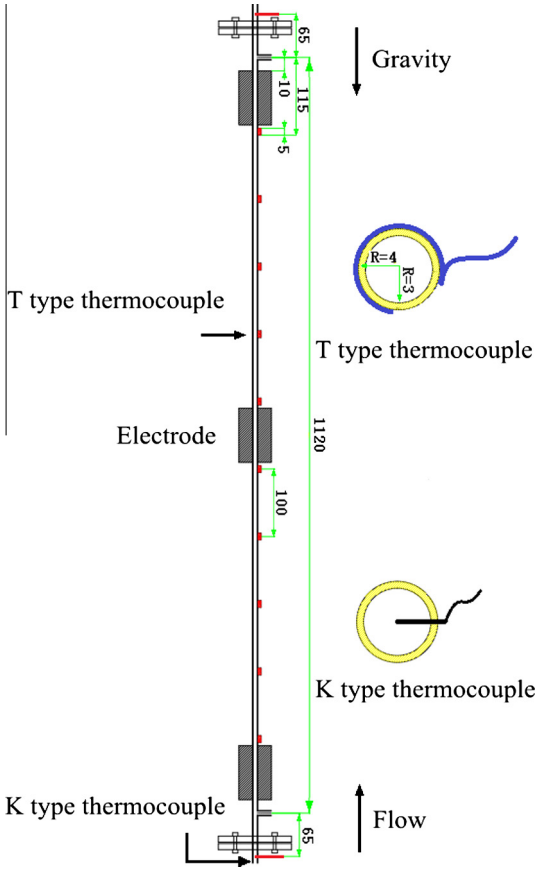

Fig. 2. Nanofluid flow boiling test section.

98% in the convective heat transfer process near saturated flow boiling in this study. During the experiment process, the temperature, differential pressure, mass flow rate and system pressure are all measured after the system has reached steady condition. The parameters of the test section and system are shown is Table 1.

The heat transfer characteristics can be descripted by heat transfer coefficient (h) and the Nusselt number (Nu):

Table 1
Parameters of the test section and system.

Parameter	Value
Length	1100 mm
Inner diameter	6 mm
Outer diameter	8 mm
Mass flux	350–1100 kg m^{-2} s^{-1}
Heat flux	48–289 kW m^{-2}
Pressure	0.2–0.8 MPa

$$Nu = \frac{hD_{in}}{k_l} = \frac{q_w D_{in}}{\Delta t_m k_l} \tag{1}$$

where q_w is the inert wall surface heat flux of the test section, and Δt_m is the logarithmic mean temperature difference. k_l is the conductivity of working fluid. The properties of nanofluid at different temperatures and concentrations are analyzed and selected in Wang's paper [5].

$$q_w = \eta \frac{Q}{\pi D_{in} l} \tag{2}$$

$$\Delta T_m = \frac{\Delta T_{max} - \Delta T_{min}}{\ln\left(\frac{\Delta T_{max}}{\Delta T_{min}}\right)} \tag{3}$$

$$\Delta T_{max} = \frac{1}{5}\sum_{i=1}^{5} T_{w,in,i} - T_{f,in} \tag{4}$$

$$\Delta T_{min} = \frac{1}{5}\sum_{i=6}^{10} T_{w,in,i} - T_{f,out} \tag{5}$$

where $T_{w,in}$ is the inner wall surface temperature, it is equivalent one dimensional cylindrical heat conduction and its heat conduction differential equation can be written as Eq. (6). Thus, the theoretical solution is shown in Eq. (8):

$$\frac{1}{r}\frac{d}{dr}\left(r\frac{dT}{dr}\right) + \frac{\dot{\Phi}}{k_s} = 0 \tag{6}$$

$$r = r_{in}, -k_s\frac{dT}{dr} = q_w; \quad r = r_{out}, \quad T = T_{w,out} \tag{7}$$

$$T_{w,in} = T_{w,out} - \left(\frac{2r_{in}q_w + r_{in}^2\dot{\Phi}}{2k_s}\right)\ln\left(\frac{r_{out}}{r_{in}}\right) - \frac{\dot{\Phi}}{4k_s}\left(r_{in}^2 - r_{out}^2\right) \quad (8)$$

where k_s is the conductivity of stainless steel, which is published in Kenneth's paper [18], and $\dot{\Phi}$ is the heat of unit volume of the tube and it can be calculated by Eq. (9):

$$\dot{\Phi} = \eta\frac{Q}{\pi(r_{out}^2 - r_{in}^2)l} \quad (9)$$

2.2. Nanofluid preparation and uncertainty analysis

In present work, acicular γ-Al_2O_3 nanoparticles with 20 nm of mean diameter and 50 nm of length and AlN nanoparticle with 30 nm of mean diameter are used to prepare nanofluid, and the based fluid is deionized water. There are three stages in preparing process. Firstly, the deionized water was weighed by an electronic scale and the density of the deionized water was measured by a densimeter to calculate its volume. After that, the mass of nanoparticle which is needed for the appointed volume concentration was calculated based on the density of nanoparticle. Secondly, the nanoparticles with appointed mass are injected into deionized water and the suspension was mechanically mixed for ten minutes. After all, the suspension was injected into the tank and an ultrasonic vibration unit is used to disperse the nanoparticles for over 24 h. So as to prevent the nanoparitcles from depositing on the wall, the pump and the ultrasonic vibration unit are working for 24 h/day at 40 kHz. Moreover, no sedimentation is found after 10 h and nanofluid density is measured every day to make sure that nanoparticles have not deposited as is shown in Fig. 3. Nanoparticle shapes are scanned by transmission electron microscope (TEM), Fig. 4 show the shapes of AlN nanoparticle before boiling.

The uncertainties of the experimental setup are reported in Table 2. In the method mentioned above, a dependent variable, named R has independent linear parameters, like $R = R\ (u_1, u_2 \ldots u_n)$. Thus, the uncertainty of R can be calculated by Eq. (11):

$$\frac{\delta R}{R} = \sqrt{\left(\frac{\delta u_1}{u_1}\right)^2 + \left(\frac{\delta u_2}{u_2}\right)^2 + \ldots + \left(\frac{\delta u_n}{u_n}\right)^2} \quad (10)$$

Moreover, for every parameter collected by the data acquisition system, its total uncertainty can be calculated by Eq. (12):

$$\frac{\delta R}{R} = \sqrt{\left(\frac{\delta R_{dau}}{R_{dau}}\right)^2 + \left(\frac{\delta R_{muu}}{R_{muu}}\right)^2} \quad (11)$$

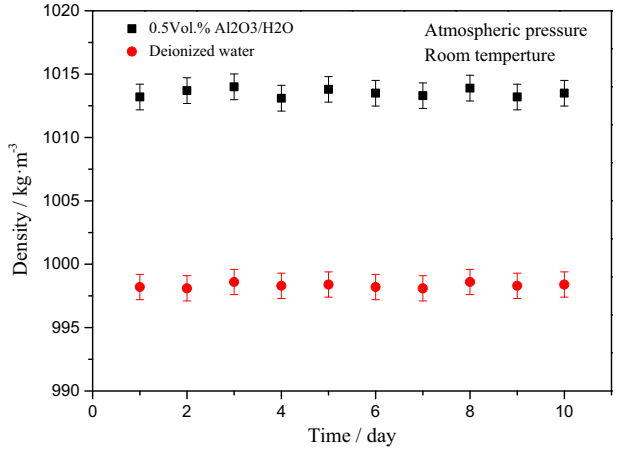

Fig. 3. The variation of nanofluid density in the experiment process.

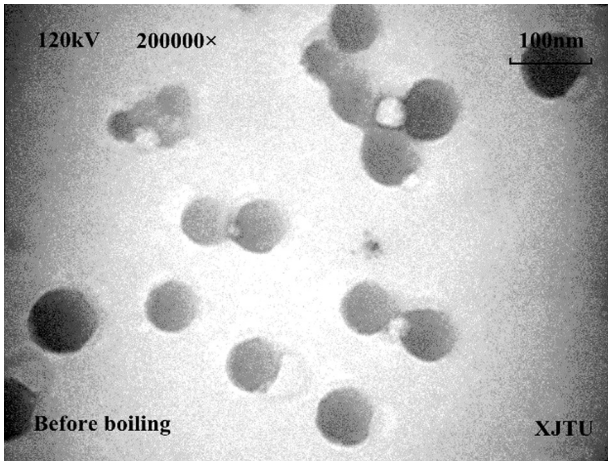

Fig. 4. TEM image of AlN nanoparticles before boiling.

Table 2
Measuring unit and their uncertainties.

Measuring parameter	Measuring unit	Uncertainty (%)
Fluid temperature	K-type sheathed thermocouple	±0.75
Wall temperature	T-type patched thermocouple	±0.75
Pressure	Pressure transmitter	±0.25
Mass flow rate	Coriolis mass flow meter	±0.2
Diameter	Vernier caliper	±0.1
Heat power	Direct reading	±0.05
Data signal	NI data acquisition system	±0.02
Length	Tape	±0.01

where R_{dau} is the data acquisition uncertainty and R_{muu} is the measuring unit uncertainty.

Thus, experimental results uncertainties can be calculated by Eqs. (1)–(11), and the calculation results are reported in Table 3.

3. Development of a correlation

3.1. Deionized water saturated flow boiling as a verification test

Some saturated flow boiling experiment were performed for deionized water to validate the accuracy and reliability of the experimental results. Fig. 5 shows the comparison between the experimental results and the prediction results by three correlations, Chen [26] (Eq. (12)), Thom [27] (Eq. (13)) and Kotepov [28] (Eq. (14)).

$$h_{TP} = h_{NB} + h_c = 0.00122S\Delta T_{sat}^{0.24}\Delta P_{sat}^{0.75}\left(\frac{k_l^{0.79}c_{p,l}^{0.45}\rho_l^{0.49}}{\sigma^{0.5}\mu_l^{0.29}h_{fg}^{0.24}\rho_G^{0.24}}\right) + 0.023\left(\frac{k_l F}{D_{in}}\right)\left(\frac{G(1-x)D_{in}}{\mu_l}\right)\left(\frac{\mu_l c_{p,l}}{k_l}\right)^{0.4} \quad (12)$$

$$\Delta T_{sat} = 22.65\left(\frac{q_w}{10^6}\right)^{0.25}e^{\frac{-p}{6.2}} \quad (13)$$

$$Nu = 141.45\left(\frac{q_w}{\rho_g h_{fg} J}\left(\frac{\rho_g}{\rho_l}\right)^{1.45}\left(\frac{h_{fg}}{c_p T_{sat}}\right)^{0.333}\right)^{0.7} Re^{0.8}Pr^{0.333} \quad (14)$$

Very well agreement between the experimental results and the three correlations were obtained. It is revealed that ±30% deviations existed, and it is acceptable for saturated flow boiling heat transfer process. Thus, the experimental data in present work are reliable and accurate.

Table 3
Uncertainties of the experimental results and calculated parameters.

Parameter	Thermal efficiency	Heat flux	Heat transfer coefficient	Nusselt number	Enhancement rate
Symbol	η	q_w	h	Nu	–
Uncertainty	±1.08%	±1.09%	±3.83%	±3.83%	±3.83%

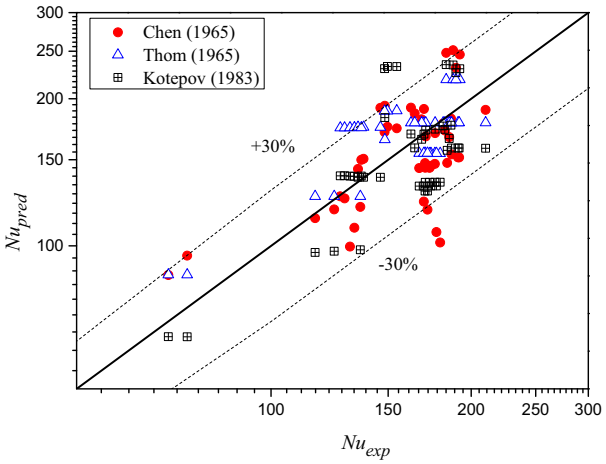

Fig. 5. Comparison between the experimental results and the prediction results.

3.2. Relevant dimensionless parameter

So as to ensure the nanoparticles haven't been changed during the experimental process, nanoparticle shapes and sizes are scanned by TEM after flow boiling experiment. As is shown in Fig. 6, it is found that the nanoparticle shapes and sizes haven't been changed significantly compared with the shapes and sizes shown in Fig. 4. Based on the research of Fukumoto [29], the mass of AlN hydrolyzed accounts for only 1.25% of the total AlN in the tank for 0.1 Vol.% nanoparticle volume concentration. In addition, $Al(OH)_3$ which is generated by the hydrolysis of AlN adhere to the AlN nanoparticle, thus, it has no significant influence on the shapes of nanoparticles as shown in Fig. 6. The hydrolysis of AlN has no significant influence on the stability and heat transfer in present work, thus, it can be ignored. In addition, the experimental section was disassembled while a type of nanofluid flow boiling experiment was accomplished and cut into two pieces by a cutter bar to capture the structure of heat surface after experiment. As is shown in Fig. 7, nanoparticles deposit on the heating surface as a layer of nanoparticles, and the roughness of the heating surface is deceased by this deposition.

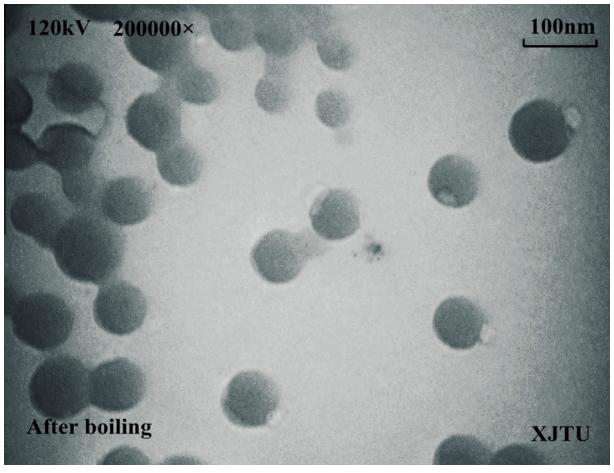

Fig. 6. TEM image of AlN nanoparticles after boiling.

The main influence factors of nanofluid saturated flow boiling include roughly heat flux on the heating surface, the system pressure, and the nanofluid thermal physical properties [22]. In present work, the effects of these factors on nanofluid saturated flow boiling are experimentally investigated. In order to propose a correlation for nanofluid saturated flow boiling, these factors were contained in several dimensionless parameters. The influence of heat flux on the heating surface can be contained in a dimensionless parameter as shown in Eq. (15). The heat flux (q) and the latent heat (h_{fg}) present the influence of the intensity of vaporization and boiling, the inner diameter of tube (D_{in}) and the viscosity of nanofluid (μ_{nf}) present the influence of the size of channel and flow characteristics. Fig. 8 shows the relationship between Nusselt number of AlN/H_2O nanofluid flow boiling and the dimensionless parameter ($q_w D_{in}/\mu_{nf} h_{fg}$) under different pressures. This dimensionless parameter has been proposed in the previous work [30].

$$\frac{q_w D_{in}}{\mu_{nf} h_{fg}} \tag{15}$$

The influence of pressure can be expressed by the difference between gas phase (steam) and liquid phase, and the dimensionless pressure can be described as the ratio between the densities of liquid phase and gas phase as shown in Eq. (16). The relationship between pressure and Nusselt number is also presented in Fig. 8. As we can see, the Nusselt numbers for the four different pressures have significant differences between each other, the Nusselt number is reduced with increasing the pressure (the ratio between the densities of liquid phase and gas phase). In addition, with the consideration of heat flux and thermal properties, the Nusselt numbers are different in similar ratios between the densities liquid phase and gas phase.

$$\frac{\rho_l}{\rho_g} \tag{16}$$

Nanoparticle random motion is a key factor for nanofluid heat transfer and it is related to temperature. For saturated flow boiling, the saturated temperatures are different for different pressures, thus, the enhancements of nanofluid inner heat transfer are different. These differences are mainly embodied in the thermal properties, especially for different nanoparticle types and volume concentrations as is shown in the previous work [30]. A dimensionless can be proposed as shown in Eq. (17) to present the influence of thermal properties. In includes nanofluid viscosity (μ_{nf}), nanofluid specific heat ($c_{p,nf}$) and nanofluid thermal conductivity (λ_{nf}).

$$\frac{\mu_{nf} c_{p,nf}}{\lambda_{nf}} \tag{17}$$

As mass flux may be an influence factor for flow boiling, the effect of mass flux on Nusselt number for 0.1 Vol.% AlN/H_2O and Al_2O_3/H_2O nanofluid are shown in Fig. 9. As we can see, the influence of mass flux was not significant both for deionized water and nanofluid in the range of this work (heat flux of 48–289 kW m^{-2}, mass flux of 350–1100 kg/m^{-2} s^{-1}) as the same as other flow boiling researches. The reason is boiling heat transfer plays a leading

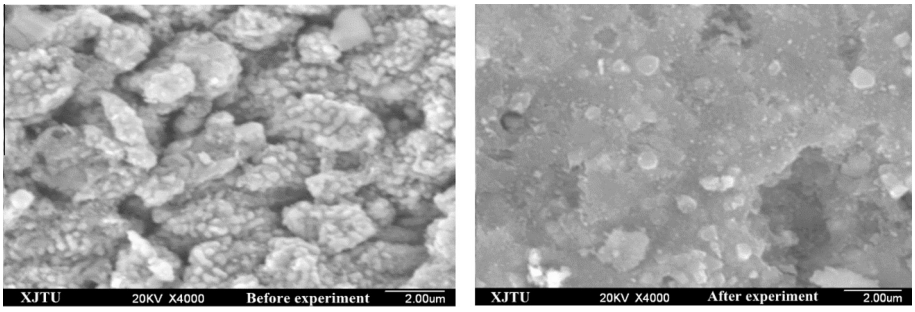

Fig. 7. SEM pictures of heating surface before and after experiment.

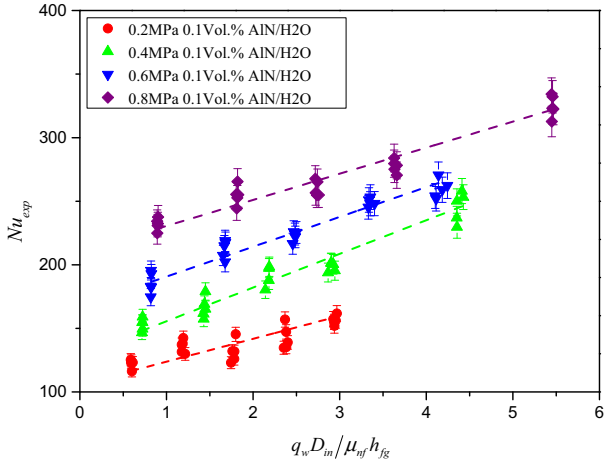

Fig. 8. Effects of dimensionless parameter and pressure on Nusselt number for 0.1 Vol.% AlN/H_2O nanofluid.

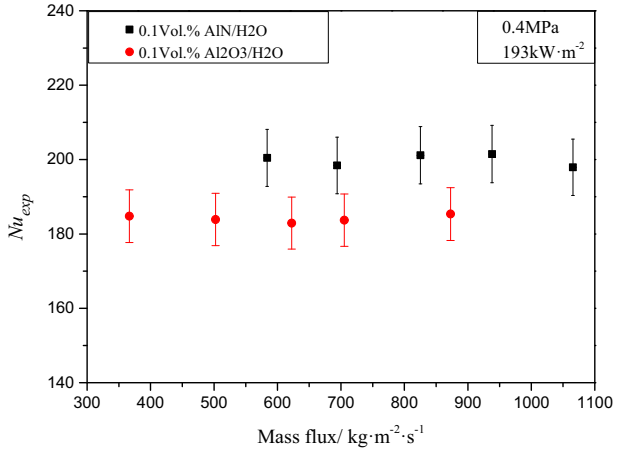

Fig. 9. Effects of mass flux on Nusselt number for 0.1 Vol.% AlN/H_2O and Al_2O_3/H_2O nanofluid.

role in the process and it is much greater than that of the convection heat transfer based on the research of Chen [26]. Thus, the correlation is proposed without the consideration of mass flux.

3.3. A correlation for nanofluid saturated flow boiling heat transfer

Based on the analysis above, a new correlation for nanofluid saturated flow boiling heat transfer can be described as followed.

$$Nu = C_1\left(\frac{q_w D_{in}}{\mu_{nf} h_{fg}}\right)^{C_2}\left(\frac{\mu_{nf} c_{p,nf}}{k_{nf}}\right)^{C_3}\left(\frac{\rho_l}{\rho_g}\right)^{C_4} \tag{18}$$

where C_1, C_2, C_3, C_4 are constants needed to be determined. Taking the common logarithm on the both sides of the equation, a new type which is a multivariate linear regression model as Eq. (19) shows.

$$lgNu = lgC_1 + C_2 lg\left(\frac{q_w D_{in}}{\mu_{nf} h_{fg}}\right) + C_3 lg\left(\frac{\mu_{nf} c_{p,nf}}{k_{nf}}\right) + C_4 lg\left(\frac{\rho_l}{\rho_g}\right) \tag{19}$$

The constant can be solved as

$$C = (A^T A)^{-1} A^T B \tag{20}$$

$$A = \begin{bmatrix} 1 & lgA_1(1) & lgA_2(1) & lgA_3(1) \\ 1 & lgA_1(2) & lgA_2(2) & lgA_3(2) \\ \cdot & \cdot & \cdot & \cdot \\ \cdot & \cdot & \cdot & \cdot \\ 1 & lgA_1(n) & lgA_2(n) & lgA_3(n) \end{bmatrix}$$

$$B = \begin{bmatrix} lgNu(1) \\ lgNu(2) \\ \cdot \\ \cdot \\ lgNu(n) \end{bmatrix} \tag{21}$$

$$C = \begin{bmatrix} lgC_1 \\ C_2 \\ C_3 \\ C_4 \end{bmatrix}$$

$$A_1 = \left(\frac{q_w D_{in}}{\mu_{nf} h_{fg}}\right) \quad A_2 = \left(\frac{\mu_{nf} c_{p,nf}}{k_{nf}}\right) \quad A_3 = \left(\frac{\rho_l}{\rho_g}\right) \tag{22}$$

where n is the number of sample data points, and in this study its value is 100. The statics parameter and analysis results are shown in Tables 4 and 5.

As A-R^2 is remove the influence of number of dimensionless parameter, this statics parameter is more accurate than that of R^2. In addition, A-R^2 approaches 1 means that the new correlation is suitable for the experimental results. And the new correlation can be written as Eq. (22), and the comparison of predicted Nusselt value by the new correlation and the experimental results are shown in Fig. 10. In addition, Fig. 11 shows the relative deviation

Table 4
Analysis results of the new correlation.

Constant	Value	Standard error
lgC_1	0.0725	2.4738
C_2	0.1848	0.0096
C_3	4.1506	3.1163
C_4	0.8871	0.9989

Table 5
Statics parameter of the new correlation.

Statistics parameters	Value
Number of points	100
Degrees of freedom	96
Residual sum of squares (R^2)	0.0571
Adjust residual sum of squares (A-R^2)	0.9594

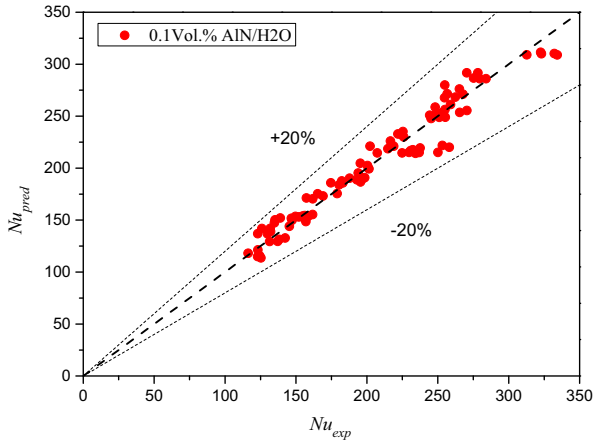

Fig. 10. Comparison of predicted *Nu* number by the new correlation and the experimental results of AlN/H_2O nanofluid.

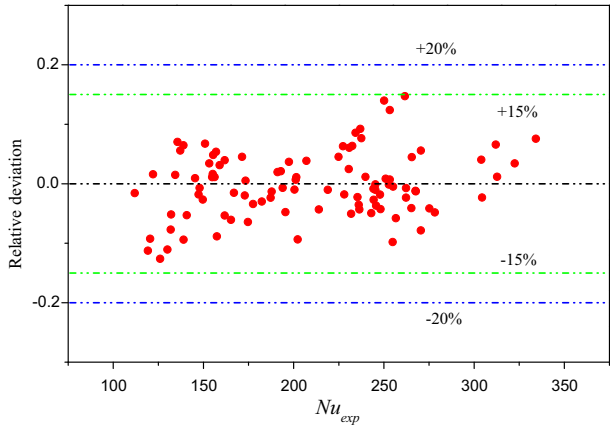

Fig. 11. Relative deviation between experiment and prediction results.

between experiment and prediction results, and it can be seen that the correlation has predicting 100% of the entire database within ±20%, 99% of the entire database within ±15%. As the mean absolute deviation (MAD) can express the average level of the prediction accuracy, it can be calculated by Eqs. (23) and (24). The mean absolute deviation of the correlation is 4.3%. Thus, the predictions agree with the measured data very well.

$$Nu = 1.1817\left(\frac{q_w D_{in}}{\mu_{nf} h_{fg}}\right)^{0.1848}\left(\frac{\mu_{nf} c_{p,nf}}{k_{nf}}\right)^{4.1506}\left(\frac{\rho_l}{\rho_g}\right)^{0.8871} \quad (23)$$

$$RD = \frac{Nu_{pred} - Nu_{exp}}{Nu_{exp}} \quad (24)$$

$$MAD = \frac{1}{N}\sum_{j=1}^{N}|RD_j| \quad (25)$$

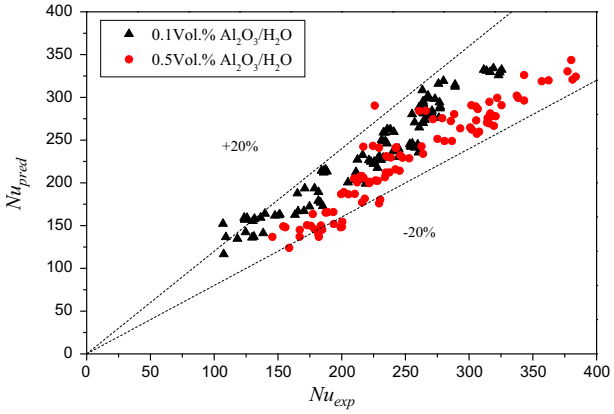

Fig. 12. Comparison of predicted *Nu* number by the new correlation and the experimental results of Al_2O_3/H_2O nanofluid.

So as to validate the new correlation and improve the range of application of the correlation, 0.1 Vol.% Al_2O_3/H_2O and 0.5 Vol.% Al_2O_3/H_2O nanofluid saturated flow boiling heat transfer are experimentally investigated, and the results are also contrasted with the prediction of the new correlation. Fig. 12 shows the comparison of predicted Nusselt number by the new correlation and the experimental results of Al_2O_3/H_2O nanofluid, and the correlation has predicting 94.5% of the entire database within ±20%. In another words, the new correlation is suitable for water based aluminum nitride and aluminum oxide nanofluid saturated flow boiling heat transfer with different volume concentrations with the range of 48–289 kW m^{-2} heat flux on the heating surface, 0.2–0.8 Mpa pressure and 350–1100 kg m^{-2} s^{-1} mass flux.

4. Conclusion

Nanofluid saturated flow boiling heat transfer in a vertical tube is experimentally investigated in this work. Nanoparticle shapes and sizes are scanned by TEM before and after boiling and it has been ensured that the nanoparticles haven't been changed during the experimental process. Several factors are under consideration, including heat flux on the heating surface, pressure and nanoparticle types and volume concentrations. After that, several relevant dimensionless parameters for nanofluid saturated flow boiling were proposed with the consideration of heat flux, pressure and thermal properties. Based on the research above, a new correlation for nanofluid saturated flow boiling was presented with 300 experimental points.

This correlation applies to both AlN/H_2O nanofluid and Al_2O_3/H_2O nanofluid (0.1–0.5 Vol.%). The pressure range of application for the correlation is 0.2–0.8 MPa, and it is 48–289 kW m^{-2} for heat flux, 350–1100 kg m^{-2} s^{-1} for mass flux. The correlation Adjust residual sum of squares (A-R^2) is 0.9594. Its mean absolute deviation (MAD) is 4.3%, and it predicts 99% of the entire database within ±15% for AlN/H_2O nanofluid and 94.5% of the entire database within ±15% for Al_2O_3/H_2O nanofluid.

Acknowledgement

The present work is supported by the National Natural Science Foundation of China (No. 51276164) and the Open Fund Program of Key Laboratory of Advanced Reactor Engineering and Safety, Ministry of Education of China.

References

[1] S.U.S. Choi, Enhancing thermal conductivity of fluids with nanoparticles, ASME-Publ.-Fed 231 (1995) 99–106.
[2] S. Suresh, P. Selvakumar, M. Chandrasekar, V. Srinivasa Raman, Experimental studies on heat transfer and friction factor characteristics of Al_2O_3/water nanofluid under turbulent flow with spiraled rod inserts, Chem. Eng. Process. Process Intensif. 53 (2012) 24–30.
[3] M.P. Beck, T.F. Sun, A.S. Teja, The thermal conductivity of alumina nanoparticles dispersed in ethylene glycol, Fluid Phase Equilib. 260 (2) (2007) 275–278.
[4] J. Lee, I. Mudawar, Assessment of the effectiveness of nanofluids for single-phase and two-phase heat transfer in micro-channels, Int. J. Heat Mass Transf. 50 (3) (2007) 452–463.
[5] Y. Wang, J.M. Wu, Numerical simulation on single bubble behavior during Al_2O_3/H_2O nanofluids flow boiling using Moving Particle Simi-implicit method, Prog. Nucl. Energy 85 (2015) 130–139.
[6] Y.P. Zhang, S.P. Niu, L.T. Zhang, et al., A review on analysis of LWR severe accident, J. Nucl. Eng. Radiat. Sci. 1 (4) (2015) 041018.
[7] G.H. Su, S.Z. Qiu, W.X. Tian, et al., Thermal Hydraulic Numerical Analysis of Nuclear Power System, Tsinghua University Press, Beijing, 2013.
[8] M. Mehrali, E. Sadeghinezhad, M.A. Rosen, S.T. Latibari, M. Mehrali, H.S.C. Metselaar, S.N. Kazi, Effect of specific surface area on convective heat transfer of graphene nanoplatelet aqueous nanofluids, Exp. Therm. Fluid Sci. 68 (2015) 100–108.
[9] A.S. Kherbeet, H.A. Mohammed, B.H. Salman, H.E. Ahmed, O.A. Alawi, M.M. Rashidi, Experimental study of nanofluid flow and heat transfer over microscale backward-and forward-facing steps, Exp. Therm. Fluid Sci. 65 (2015) 13–21.
[10] M.M. Sarafraz, F. Hormozi, Heat transfer, pressure drop and fouling studies of multi-walled carbon nanotube nano-fluids inside a plate heat exchanger, Exp. Therm. Fluid Sci. 72 (2016) 1–11.
[11] D. Huang, Z. Wu, B. Sunden, Effects of hybrid nanofluid mixture in plate heat exchangers, Exp. Therm. Fluid Sci. 72 (2016) 190–196.
[12] R. Barzegarian, M.K. Moraveji, A. Aloueyan, Experimental investigation on heat transfer characteristics and pressure drop of BPHE (brazed plate heat exchanger) using TiO_2–water nanofluid, Exp. Therm. Fluid Sci. 74 (2016) 11–18.
[13] M.M. Sarafraz, F. Hormozi, S.M. Peyghambarzadeh, Pool boiling heat transfer to aqueous alumina nano-fluids on the plain and concentric circular micro-structured (CCM) surfaces, Exp. Therm. Fluid Sci. 72 (2016) 125–139.
[14] D. Faukner, M. Khotan, R. Shekarriz, Practical design of a 1000 W/cm^2 cooling system, in: Proc. of 19th IEEE SEMI-THERM Symposium, San Jose, CA, 2003, pp. 223–230.
[15] H. Peng, G.L. Ding, W.T. Jiang, H.T. Hu, Y.F. Gao, Heat transfer characteristics of refrigerant-based nanofluid flow boiling inside a horizontal smooth tube, Int. J. Refrig. 32 (2009) 1259–1270.
[16] C.S. Coursey, J. Kim, Nanofluid boiling: the effect of surface wettability, Int. J. Heat Fluid Flow 29 (2008) 1577–1585.
[17] S.J. Kim, T. McKrell, J. Buongiorno, L.W. Hu, Alumina nanoparticles enhance the flow boiling critical heat flux of water at low pressure, J. Heat Trans. 130 (2008) 044501.
[18] S.J. Kim, T. McKrell, J. Buongiorno, L.W. Hu, Subcooled flow boiling heat transfer of dilute alumina, zinc oxide, and diamond nanofluids at atmospheric pressure, Nucl. Eng. Des. 240 (2010) 1186–1194.
[19] M. Boudouh, H.L. Gualous, M. De Labachelerie, Local convective boiling heat transfer and pressure drop of nanofluid in narrow rectangular channels, Appl. Therm. Eng. 30 (17–18) (2010) 2619–2631.
[20] L. Xu, J. Xu, Nanofluid stabilizes and enhances convective boiling heat transfer in a single microchannel, Int. J. Heat Mass Transf. 55 (21e22) (2012) 5673–5686.
[21] K.B. Rana, A.K. Rajvanshi, G.D. Agrawal, A visualization study of flow boiling heat transfer with nanofluids, J. Vis. 16 (2) (2013) 133–143.
[22] K.B. Rana, G.D. Agrawal, J. Mathura, U. Puli, Measurement of void fraction in flow boiling of ZnO-water nanofluids using image processing technique, Nucl. Eng. Des. 270 (2014) 217–226.
[23] B. Sun, D. Yang, Flow boiling heat transfer characteristics of nano-refrigerants in a horizontal tube, Int. J. Refrig. 38 (2014) 206–214.
[24] E. Abedini, A. Behzadmehr, H. Rajabnia, S.M.H. Sarvari, S.H. Mansouri, Numerical investigation of subcooled flow boiling of a nanofluid, Int. J. Therm. Sci. 64 (2013) 232–239.
[25] J.M. Wu, J. Zhao, A review of nanofluid heat transfer and critical heat flux enhancement – research gap to engineering application, Prog. Nucl. Energy 66 (2013) 13–24.
[26] J.C. Chen, A correlation for boiling heat transfer to saturated fluids in convective flow, Int. Eng. Chem. Proc. Des. Dev. 5 (3) (1966) 322–329.
[27] J.R.S. Thom, Paper 6. System on Boiling Heat Transfer in Steam Generating Units and Heat Exchangers, 1965, pp. 15–16.
[28] A.M. Kotepov, Fluid Dynamics and Heat Transfer in Steam Generating, China Water Power Press, 1983, pp. 224–232.
[29] S. Fukumoto, T. Hookabe, H. Tsubakino, Hydrolysis behavior of aluminum nitride in various solutions, J. Mater. Sci. 35 (11) (2000) 2743–2748.
[30] Y. Wang, G.H. Su, Experimental investigation on nanofluid flow boiling heat transfer in a vertical tube under different pressure conditions, Exp. Therm. Fluid Sci. 77 (2016) 116–123.